VIP Single-Molecule Studies

DOI: 10.1002/anie.201007084

# Watching the Annealing Process One Polymer Chain at a Time**

*Jan Vogelsang,* Johanna Brazard, Takuji Adachi, Joshua C. Bolinger, and Paul F. Barbara†*

Annealing (i.e. equilibrating) of conjugated polymer and polymer blend films is a widely used process that achieves optimal film morphology and therefore improves material properties such as electrical mobility for photovoltaic devices and other applications.[1–7] Especially, solvent vapor annealing (SVA) is an industrially important technique since it causes a rapid morphological equilibration of films at room temperature without thermal damage of the material or other complications which are disadvantages of high-temperature annealing.[8–10] However, due to the complexity of polymer films, the understanding of SVA at the molecular level remains largely unclear. In particular, the polymer chain conformation (i.e. morphology) of the intermediates along the annealing pathway, the dynamics of chain reassembly during annealing, and spatial and temporal inhomogeneities of the annealing process have not yet been determined. A better understanding of SVA at the molecular level could lead to improved processing methods of conjugated polymer films, and even to the first rational design approaches for this material class. Single molecule fluorescence spectroscopy/microscopy (SMS) techniques are a promising approach to obtain a molecular picture of SVA and have already proven to be a valuable experimental tool to study conjugated polymer chain conformations.[11–17]

Herein, we report the real-time observation of morphological dynamics induced by SVA in a model system comprised of single chains of a prototypical conjugated polymer poly(2-methoxy-5-(2′-ethylhexyloxy)-1,4-phenylene-vinylene) (MEH-PPV; denoted here as single CP chains) embedded in a poly(methyl methacrylate) (PMMA) host matrix. SMS techniques using a home-built gas/solvent vapor flow chamber (see Experimental Section for details) enabled us to monitor the SVA-induced translocations of single chains (Figure 1), to observe the dynamics of chains folding and unfolding (Figure 2), and to compare morphological order in single chains immediately after spin-coating of a film to ones after SVA (Figure 3).

The main results are summarized in Scheme 1. Ensemble spectroscopic measurements have shown that CP chains in the solvents used here are isolated, well solvated, and contain

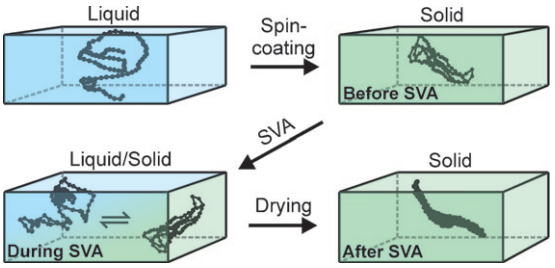


***Scheme 1.*** Connection between the conjugated polymer chain conformation and the phase of the sample (SVA, solvent vapor annealing).

few, if any, intra-chain contacts.[18–20] In a spin-coated MEH-PPV/PMMA film, SMS data show a heterogeneous distribution of collapsed CP chain conformations, including subpopulations of relatively disordered conformations that are kinetically trapped in a high energy state and ordered conformations with a low energy state. During SVA, the film resides in a heterogeneous mixture of solid and liquid-like phase in which the CP chains undergo folding/unfolding events between a collapsed and an extended conformation. The CP chains also undergo large translational jumps during SVA. When SVA is terminated, a solid MEH-PPV/PMMA film is produced in which the CP chains are exclusively in equilibrated highly ordered conformations.

Figure 1 shows typical fluorescence images before (Figure 1a), during (Figure 1b), and after (Figure 1c) SVA of a MEH-PPV/PMMA film. Stationary single CP chains can be observed in the long exposure images (ca. 180 s) in Figure 1a and c as diffraction-limited fluorescence spots. In contrast, during SVA, the translational diffusion of CP chains is observed in Figure 1b as elongated and blurred fluorescence spots and an increase of fluorescence in the background. A movie corresponding to Figure 1b (Movie S1) and additional information are available in the Supporting Information. Swelling of PMMA by toluene vapor has been studied previously and it was reported that absorption of saturated toluene vapor effectively lowers the glass transition temperature, $T_G$, of high molecular weight PMMA from about 390 K to near or below ambient temperature.[21,22] The observed translational diffusion of single CP chains is clearly due to PMMA swelling. During SVA, the observed single CP chain position trajectories, such as the inset in Figure 1b, reveal large fluctuations in the apparent diffusion coefficient, which can, at our level, be sorted into three time regimes. These

[*] Dr. J. Vogelsang, Dr. J. Brazard, T. Adachi, Dr. J. C. Bolinger, Prof. Dr. P. F. Barbara
Center for Nano and Molecular Science and Technology and Department of Chemistry and Biochemistry
The University of Texas at Austin, Austin, TX 78712 (USA)
Fax: (+1) 512-471-3389
E-mail: jvogelsang@mail.utexas.edu

[†] Deceased

[**] This work was supported by the program "Understanding Charge Separation and Transfer at Interfaces in Energy Materials and Devices (EFRC:CST)", an Energy Frontier Research Center funded by the U.S. Department of Energy, Office of Science, Office of Basic Energy Sciences under Award Number DE-SC0001091. J.V. thanks the German Research Foundation (DFG) for a fellowship.

Supporting information for this article is available on the WWW under http://dx.doi.org/10.1002/anie.201007084.

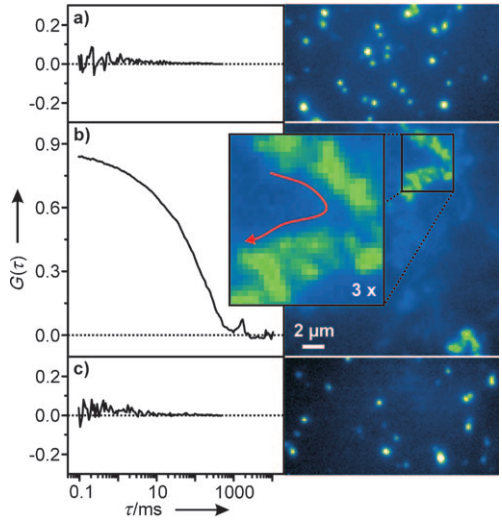


***Figure 1.*** Fluorescence correlation spectroscopy (FCS) and wide-field fluorescence images of MEH-PPV/PMMA thin films are presented under different processing conditions. Left: FCS curves acquired from a PMMA film with an average concentration of MEH-PPV of approximately 1 molecule $\mu m^{-2}$ a) before, b) during, and c) after SVA. Right: Wide-field fluorescence images of a PMMA film containing isolated MEH-PPV molecules a) before, b) during, and c) after SVA. The red arrow corresponds to a molecule which undergoes translation. The images are averaged over 180 images with an integration time of 1 s each. The excitation intensity was approximately 1 $W cm^{-2}$.

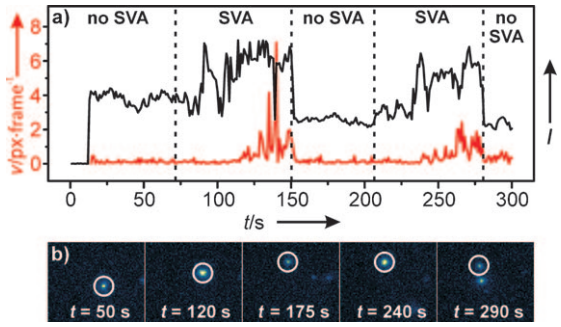


***Figure 2.*** Fluorescence intensity transient of a single MEH-PPV molecule within a PMMA host matrix during nitrogen purging (no SVA) and solvent vapor annealing (SVA). a) The complete fluorescence transient (black curve) and the velocity, $v$, (red curve) can be recorded by tracking the position of the spot. b) Wide-field fluorescence images corresponding to the fluorescence transient in (a) at the times indicated.

fluctuations range from: 1) stationary positions on the seconds time scale, 2) time resolvable translocations between 100 ms and 1 s, and 3) rapid "liquid"-like diffusion on the 1–100 ms timescale. The CP chains in the "liquid"-like domains move too fast to be observed directly in the wide-field microscope images but are clearly detectable by fluorescence correlation spectroscopy (FCS). The FCS curves in Figure 1 show that a large amplitude of intensity fluctuations is observed on the 10–100 ms timescale during SVA due to translation through the diffraction-limited FCS excitation/observation volume (Figure 1 b), while no significant motion is observed before and after exposing the film to solvent vapor (Figure 1 a,c). A high heterogeneity of diffusion times was also observed during the polymerization process of a polymer network and it was concluded that the different diffusion times are related to different degrees of network formation in space.[23] Since the formation and disintegration of a polymer network is related to swelling, a spatial heterogeneous swelling process can be assumed here during SVA.

Conformational changes that occur to the CP chains involving the unfolding and folding correlated with SVA were observed as fluorescence intensity fluctuations (Figure 2 and Figure S1). The fluorescence transients of single CP chains were measured by wide-field fluorescence microscopy over a long time period (200–300 s) while the environment was switched between SVA and pure $N_2$ (no SVA) as indicated in Figure 2 a and Figure S1 (see also Movie S2 which corresponds to the transient in Figure 2). Due to the translation of single CP chains during SVA the fluorescence intensity transients were acquired by tracking the diffraction-limited fluorescence spots under both static and annealing conditions. Additionally, wide-field fluorescence images of a CP chain corresponding to the fluorescence transient at various times and different conditions are presented (Figure 2 b). The fluorescence transients show that the intensity of single CP chains under SVA is two to three times higher compared to conditions with no solvent vapor present (no SVA). Since over the complete acquisition time the same single CP chain is observed and therefore no change in the absorption cross-section can be assumed, this intensity increase is clearly due to an increase in the quantum yield of fluorescence, $\phi_{FI}$.

It has been known from ensemble spectroscopy measurements that the $\phi_{FI}$ of MEH-PPV decreases by a factor of 2–3 from solutions compared to films.[24,25] The $\phi_{FI}$ decrease is due to the conformational transition of CP chains from an extended conformation to a collapsed conformation.[20] Nguyen et al. reported the correlation between the hydrodynamic radius of MEH-PPV chains and their $\phi_{FI}$ value by comparing the results of dynamic light scattering experiments and $\phi_{FI}$ measurements in different solvents. The hydrodynamic radius decreases in the poor solvent tetrahydrofuran (THF) compared to the good solvent chlorobenzene. The $\phi_{FI}$ of MEH-PPV is lower in the poor solvent compared to the good solvent, suggesting that $\phi_{FI}$ is lower in a more collapsed conformation.[20] Therefore we conclude that the observation of the intensity change is due to the transition between a collapsed and an extended conformation, although the mechanism of self-quenching is still unclear. Additionally, the switching between these two conformations is reversible as shown in Figure 2 with two switching cycles shown here for a single CP chain.

The red curve in Figure 2 a plots the velocity of the translational diffusion, which was measured as the shift of the centroid position of the fluorescence spot between two consecutive images. The correlation between the intensity increase, translational motion and SVA further indicates that the intensity increase occurs in the solid/liquid-like phase of PMMA. A low excitation intensity was employed (1 $W cm^{-2}$) to avoid photophysical artifacts such as blinking and photobleaching, and therefore limited the temporal resolution in

  

the measurements (1 s integration time). For these reasons, we were only able to observe intensity changes for slowly moving CP chains. A majority of CP chains diffuses out of the excitation area before an intensity increase can be recorded, and approximately 10% of the CP chains remain in the excitation area and they demonstrate an intensity increase before any translational movement occurs like the data shown in Figure 2. This indicates that unfolding can occur even before the network of the surrounding host matrix is substantially swollen, and the heterogeneity of the swelling process of the PMMA matrix leads to different diffusion coefficients as observed in Figure 1. Further examples of an intensity increase during SVA due to unfolding are shown in Figure S1 and it is also observed in a MEH-PPV bulk film (Figure S2).

Finally, by using fluorescence excitation polarization spectroscopy, it is revealed that in fact SVA equilibrates the conformation of single CP chains towards a lower-energy, highly ordered conformation (Figure 3). Hu et al. showed that this spectroscopic technique can be used on single CP chains to characterize the conformational order through the polarization excitation anisotropy, $A$.[11] The fluorescence intensity of single CP chains was measured while rotating the angle of the linearly polarized excitation light in the $x$–$y$ plane of the laboratory frame. The modulation depth, $M$, was obtained by fitting Equation (1) to the intensity vs. polarization angle, $\theta$, where $\phi$ is the orientation of the net dipole moment of the polymer chain, when the emission is maximized.

$$I(\theta) \propto 1 + M\cos 2(\theta - \Phi) \quad (1)$$

For each single CP chain, $M$ was acquired and a histogram over a large number of CP chains (see caption of Figure 3 for details) was obtained (Figure 3a–d). Since $M$ is only a projection of $A$ onto the $x$–$y$ plane, we used a model which takes the 3-dimensional and randomly distributed orientations of the CP chains as well as optical effects of the microscope into account to extract an excitation anisotropy histogram. Here an empirical Gaussian or bi-Gaussian distribution was employed. Details on the experimental setup, data acquisition, and analysis are described elsewhere.[17]

It has been shown that the majority of single MEH-PPV chains fold into highly ordered conformations in PMMA when a film is spin-coated from toluene.[17] Nearly identical results are demonstrated here using a sample purified by gel permeation chromatography (GPC) (Figure 3a). The modulation depth histogram for the sample spin-coated from toluene shows few low values, but primarily values above 0.5 with a mean modulation depth of 0.7. This modulation depth histogram including the lower values can be well described by a Gaussian distribution of $A$ values (Figure S3a) with a mean of 0.81 and a standard deviation of 0.12 (Figure 3e, dotted curve). In contrast, a sample deposited from chloroform shows a broader modulation depth histogram (Figure 3b) that can only be sufficiently described by at least a bi-Gaussian distribution (Figure S3b), with mean values of 0.52 and 0.84 and standard deviations of 0.11 and 0.09, respectively (Figure 3f, dotted curve).

These samples were additionally solvent vapor annealed for 60 min with nitrogen gas saturated with toluene. After SVA, a striking change in the modulation depth histograms was probed by excitation polarization fluorescence spectroscopy. Both samples spun from toluene and chloroform following SVA demonstrate a sharper distribution compared to the samples before SVA (Figure 3c,d). Very similar single Gaussian anisotropy distributions are extracted for both samples with a mean of 0.83 and a standard deviation of 0.07 for the sample spin-coated from toluene and a mean of 0.90 and a standard deviation of 0.1 for the sample spin-coated from chloroform, respectively (Figure 3e,f black curves). Possible conformations, which would lead to the measured mean values are presented as insets in Figure 3a–d to illustrate the conformational change. The number of detected spots, the intensity of the spots, and the film thickness (as measured by atomic force microscopy, see Figure S4) remain the same before and after SVA. These similar pre- and post-SVA results demonstrate that within the time scale of the experiment aggregation, dissociation, photo degeneration, and de-wetting can be neglected during the SVA process.

Additional studies of SVA with chloroform- instead of toluene-saturated gas reveal similar trends in the anisotropy distribution for a sample spin-coated from chloroform (Fig-

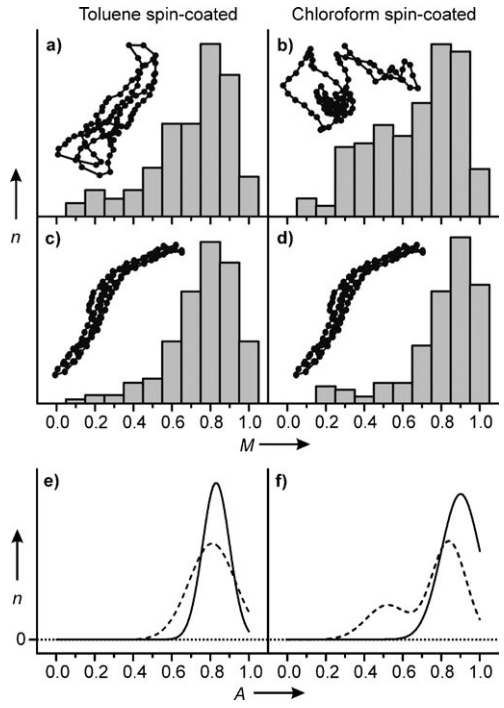


***Figure 3.*** The experimental histograms of modulation depth, $M$, from single MEH-PPV molecules (number average molecular weight 830 kDa) embedded in a PMMA host matrix with different preparation methods: Spin-coated from a) toluene and b) chloroform solution. c,d) The samples were additionally solvent vapor annealed for 60 min with toluene-saturated nitrogen gas. The histograms consist of 152, 230, 160, and 146 MEH-PPV molecules for (a), (b), (c), and (d), respectively. The insets illustrate a conformation of the molecule consistent with the histograms average. e,f) Anisotropy, $A$, distributions before (-----) and after SVA (——) resolved by the best fit for (a)–(d), which generated the data shown in Figure S3 (striped graphs).

  

ure S5). The obtained values for the Gaussian anisotropy distributions after SVA with toluene and chloroform (mean of 0.9 and standard deviation of 0.1 for toluene SVA, mean of 0.87 and standard deviation of 0.16 for chloroform SVA) indicate little dependency on the solvent used for SVA as long as the solubility of MEH-PPV/PMMA and the solvent vapor is sufficient. In contrast, the solubility of PMMA in hexane is limited, and control experiments with hexane-saturated gas reveal no changes during and after SVA. These data reveal that the influence of solvents used for the spin-coating process on the conformation of single CP chains is minimized or eliminated after SVA with good solvents, allowing the chains to fold into low-energy, highly ordered conformations upon SVA. It has been reported that single CP chains in a PMMA matrix spin-coated from chloroform produces disordered conformations while toluene produces more ordered conformations, for which the reason is still under discussions.[26] Since both toluene and chloroform SVA produces low-energy, highly ordered conformations but different conformations upon spin-coating, we suggest that the increased disorder in samples spin-coated from chloroform can be attributed to the lower boiling point of chloroform (334 K) compared to toluene (383 K). The evaporation rate during the spin-coating process is higher for the lower boiling point solvent, which leads to a higher probability of trapping the CP chains in a high-energy, disordered conformation. For example it was shown that a high rotation speed (8000 rpm) during the spin-coating process of bulk MEH-PPV films leads to a high evaporation rate of the solvent, and it was observed that the CP chains become kinetically trapped in their solvent configuration.[27]

Solvent vapor annealing is one of the most important industrial techniques used to improve device properties such as the efficiency of organic solar cells, but little is known about the molecular details of SVA. Herein, we prove that single-molecule fluorescence spectroscopy is capable of giving us a fundamental understanding of SVA on the molecular level. It was shown that SVA in fact equilibrates the conformation of CP chains even though the CP chains are trapped in a high-energy, disordered conformation prior to SVA due to the use of spin-coating with different solvents. SMS also enabled us to study the details of the SVA process. During SVA, the film absorbs solvent lowering the glass transition temperature below the ambient temperature, and translational motion of the CP chains can be observed within this solid/liquid-like film. Further, it was shown that the CP chains undergo folding and unfolding events between a collapsed and extended conformation during SVA, which finally leads to a lower-energy, highly ordered conformation after the solvent vapor is removed.

## Experimental Section

Poly(2-methoxy-5-(2′-ethylhexyloxy)1,4-phenylenevinylene) (MEH-PPV) was purchased from Polymer Source Inc. and further purified by GPC with a polystyrene standard to obtain $M_n = 830$ kDa with a PDI of 3.5. Poly(methyl methacrylate) (PMMA, $M_n = 45$ kDa, PDI = 2.2) was purchased from Sigma Aldrich Co. Glass coverslips were cleaned in an acid piranha solution (hydrogen peroxide/sulfuric acid 1:3 in volume). Isolated chains of MEH-PPV embedded in a PMMA matrix were obtained by dynamically spin-coating from toluene or chloroform. The PMMA film thickness was 200 nm, and the concentration of MEH-PPV in solution before spin-coating was approximately $10^{-13}$ mol L$^{-1}$, leading to a final spot density of about 0.1 spots μm$^{-2}$. To avoid any photo-oxidation of samples, they were prepared in a glove box (MBraun, with $O_2$ and $H_2O$ less than 5 ppm) and investigated in the microscope apparatus (see Supporting Information) equipped with a home-built gas flow cell to purge the sample with nitrogen gas, preventing exposure of the sample to oxygen or moisture. The removal of oxygen was examined by applying high-intensity pulses on single conjugated polymer chains, which leads to a significant triplet build-up if no oxygen is present (see Figure S6 and Ref. [28] for details). For SVA the nitrogen gas was saturated with the respective solvent (toluene, chloroform, or hexane) by slowly purging the gas through a reservoir of the solvent. For the preparation of the bulk MEH-PPV film a concentrated MEH-PPV/THF solution ($10^{-7}$–$10^{-8}$ mol L$^{-1}$) was spin-cast at 2000 rpm onto a glass substrate.

Received: November 11, 2010
Published online: February 3, 2011

**Keywords:** annealing · conjugated polymers · polarization spectroscopy · polymer morphology · single-molecule studies

[1] M. Granstrom, K. Petritsch, A. C. Arias, A. Lux, M. R. Andersson, R. H. Friend, *Nature* **1998**, *395*, 257.
[2] H. Sirringhaus, P. J. Brown, R. H. Friend, M. M. Nielsen, K. Bechgaard, B. M. W. Langeveld-Voss, A. J. H. Spiering, R. A. J. Janssen, E. W. Meijer, P. Herwig, D. M. de Leeuw, *Nature* **1999**, *401*, 685.
[3] T. Q. Nguyen, I. B. Martini, J. Liu, B. J. Schwartz, *J. Phys. Chem. B* **2000**, *104*, 237.
[4] W. L. Ma, C. Y. Yang, X. Gong, K. Lee, A. J. Heeger, *Adv. Funct. Mater.* **2005**, *15*, 1617.
[5] R. J. Kline, M. D. McGehee, E. N. Kadnikova, J. S. Liu, J. M. J. Frechet, M. F. Toney, *Macromolecules* **2005**, *38*, 3312.
[6] M. Reyes-Reyes, K. Kim, D. L. Carroll, *Appl. Phys. Lett.* **2005**, *87*, 083506.
[7] X. N. Yang, J. Loos, S. C. Veenstra, W. J. H. Verhees, M. M. Wienk, J. M. Kroon, M. A. J. Michels, R. A. J. Janssen, *Nano Lett.* **2005**, *5*, 579.
[8] A. M. Hor, R. O. Loutfy, *Thin Solid Films* **1983**, *106*, 291.
[9] K. Y. Law, *Chem. Rev.* **1993**, *93*, 449.
[10] S. Miller, G. Fanchini, Y. Y. Lin, C. Li, C. W. Chen, W. F. Su, M. Chhowalla, *J. Mater. Chem.* **2008**, *18*, 306.
[11] D. H. Hu, J. Yu, K. Wong, B. Bagchi, P. J. Rossky, P. F. Barbara, *Nature* **2000**, *405*, 1030.
[12] P. F. Barbara, A. J. Gesquiere, S. J. Park, Y. J. Lee, *Acc. Chem. Res.* **2005**, *38*, 602.
[13] B. Muls, H. Uji-i, S. Melnikov, A. Moussa, W. Verheijen, J. P. Soumillion, J. Josemon, K. Müllen, J. Hofkens, *ChemPhysChem* **2005**, *6*, 2286.
[14] D. Wöll, E. Braeken, A. Deres, F. C. De Schryver, H. Uji-i, J. Hofkens, *Chem. Soc. Rev.* **2009**, *38*, 313.
[15] F. Laquai, Y. S. Park, J. J. Kim, T. Basche, *Macromol. Rapid Commun.* **2009**, *30*, 1203.
[16] J. M. Lupton, *Adv. Mater.* **2010**, *22*, 1689.
[17] T. Adachi, J. Brazard, P. Chokshi, V. Ganesan, J. C. Bolinger, P. F. Barbara, *J. Phys. Chem. C* **2010**, *114*, 20896.
[18] R. Traiphol, P. Sanguansat, T. Srikhirin, T. Kerdcharoen, T. Osotchan, *Macromolecules* **2006**, *39*, 1165.

  

[19] E. Aharon, S. Breuer, F. Jaiser, A. Kohler, G. L. Frey, *ChemPhysChem* **2008**, *9*, 1430.
[20] T. Q. Nguyen, V. Doan, B. J. Schwartz, *J. Chem. Phys.* **1999**, *110*, 4068.
[21] T. S. Chow, *Macromolecules* **1980**, *13*, 362.
[22] F. Doumenc, H. Bodiguel, B. Guerrier, *Eur. Phys. J. E* **2008**, *27*, 3.
[23] D. Wöll, H. Uji-I, T. Schnitzler, J. I. Hotta, P. Dedecker, A. Herrmann, F. C. De Schryver, K. Müllen, J. Hofkens, *Angew. Chem.* **2008**, *120*, 795; *Angew. Chem. Int. Ed.* **2008**, *47*, 783.
[24] N. C. Greenham, I. D. W. Samuel, G. R. Hayes, R. T. Phillips, Y. Kessener, S. C. Moratti, A. B. Holmes, R. H. Friend, *Chem. Phys. Lett.* **1995**, *241*, 89.
[25] H. Lin, Y. Tian, K. Zapadka, G. Persson, D. Thomsson, O. Mirzov, P.-O. Larsson, J. Widengren, I. G. Scheblykin, *Nano Lett.* **2009**, *9*, 4456.
[26] O. Mirzov, R. Bloem, P. R. Hania, D. Thomsson, H. Z. Lin, I. G. Scheblykin, *Small* **2009**, *5*, 1877.
[27] I. M. Craig, C. J. Tassone, S. H. Tolbert, B. J. Schwartz, *J. Chem. Phys.* **2010**, *133*, 044901.
[28] A. J. Gesquiere, Y. J. Lee, J. Yu, P. F. Barbara, *J. Phys. Chem. B* **2005**, *109*, 12366.

  